JACS
JOURNAL OF THE AMERICAN CHEMICAL SOCIETY
Article
pubs.acs.org/JACS

A New ONO^{3-} Trianionic Pincer-Type Ligand for Generating Highly Nucleophilic Metal−Carbon Multiple Bonds

Matthew E. O'Reilly, Ion Ghiviriga, Khalil A. Abboud, and Adam S. Veige*

Department of Chemistry, Center for Catalysis, University of Florida, P.O. Box 117200, Gainesville, Florida 32611, United States

Supporting Information

ABSTRACT: Appending an amine to a C═C double bond drastically increases the nucleophilicity of the β-carbon atom of the alkene to form an enamine. In this report, we present the synthesis and characterization of a novel CF_3−ONO^{3-} trianionic pincer-type ligand, rationally designed to mimic enamines within a metal coordination sphere. Presented is a synthetic strategy to create enhanced nucleophilic tungsten−alkylidene and −alkylidyne complexes. Specifically, we present the synthesis and characterization of the new CF_3−ONO^{3-} trianionic pincer tungsten−alkylidene [CF_3−ONO]W═CH(Et)(O^tBu) (**2**) and −alkylidyne {$MePPh_3$}{[CF_3−ONO]W≡C(Et)(O^tBu)} (**3**) complexes. Characterization involves a combination of multinuclear NMR spectroscopy, combustion analysis, DFT computations, and single crystal X-ray analysis for complexes **2** and **3**. Exhibiting unique nucleophilic reactivity, **3** reacts with MeOTf to yield [CF_3−ONO]W═C(Me)(Et)(O^tBu) (**4**), but the bulkier Me_3SiOTf silylates the *tert*-butoxide, which subsequently undergoes isobutylene expulsion to form [CF_3−ONO]W═CH(Et)($OSiMe_3$) (**5**). A DFT calculation performed on a model complex of **3**, namely, [CF_3−ONO]W≡C(Et)(O^tBu) (**3′**), reveals the amide participates in an enamine-type bonding combination. For complex **2**, the Lewis acids MeOTf, Me_3SiOTf, and $B(C_6F_5)_3$ catalyze isobutylene expulsion to yield the tungsten−oxo complex [CF_3−ONO]W(O)(^{n}Pr) (**6**).

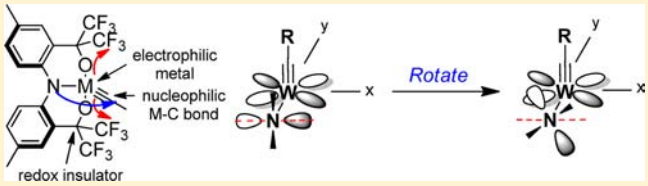

INTRODUCTION

Transition-metal multiple bonds of groups 4 and 5, in particular the first row derivatives, have a significant ionic component[1−5] and are highly nucleophilic.[1,2,5−7] Superlative examples include the alkylaluminum stabilized Tebbe's reagents ($Cp_2Ti(\mu$-$CH_2)(\mu$-X)Al(CH_3)$_2$ (X = Cl, Me)[8−11] and recently Mindiola's titanium ([PNP]Ti≡C^{t}Bu)[12−21] and vanadium ([nacnac]V≡C^{t}Bu) alkylidynes.[22,23] In contrast, group 6 metal−carbon multiple bonds[24] of molybdenum and tungsten are more covalent and correspondingly less nucleophilic.[1,3−5] However, appropriate ancillary ligand design provides the possibility to fine-tune the electronic structure of molybdenum and tungsten multiple bonds to create highly nucleophilic species. Methodologies that accentuate the nucleophilicity of M−C multiple bonds are important for applications in 1,2-CH bond activation and olefin and alkyne metathesis. Herein, we present a rational approach to creating tungsten−carbon multiple bonds with high nucleophilicity at the carbon by employing a push−pull strategy that exploits an enamine bonding concept for the push.

To create a highly nucleophilic polarized metal−carbon bond, the ancillary ligand must accentuate the electrophilicity of the metal and impart nucleophilicity to the α-carbon, a so-called push−pull effect.[25] However, inducing an electronically unsaturated metal center actually serves to diminish the nucleophilicity at the α-carbon by forming a more covalent M−C multiple bond. The challenge in polarizing the M−C bond lies in accumulating electron density on the α-carbon while removing it from the metal center.

Some of the most highly active alkene[26,27] and alkyne[28−33] metathesis catalysts employ a push−pull idea by including electron-rich imido or amido ligands coupled with electronically poor fluorinated alkoxides (−OC(CF_3)$_2$$CH_3$). The fluorinated alkoxides serve to weaken the alkoxide donor strength and create an electrophilic metal, but the role of the imido or amido is not as clear.[31,34] For monodentate amido ligands, the lone pair on the nitrogen typically orients perpendicular to the metal−carbon multiple bond and donates into a low-lying vacant d_{xy} orbital (Figure 1, left).[29,31,32,35−37] Donating electron

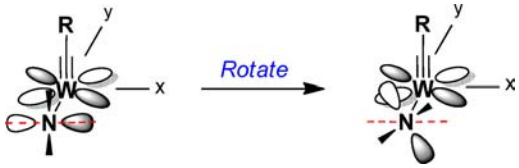

Figure 1. Left: amido p-orbital aligned with d_{xy}. Right: amido p-orbital rotated out of alignment.

density into an empty d_{xy} orbital stabilizes the N-atom lone-pair but operates against the goal of creating an electrophilic metal ion. A different strategy is to purposely orient the amido lone pair collinear or closely aligned with the metal−carbon bond axis (Figure 1, right). The result delocalizes the N-atom lone

Received: March 14, 2012
Published: June 8, 2012

dx.doi.org/10.1021/ja302222s | J. Am. Chem. Soc. 2012, 134, 11185−11195

pair through the metal−carbon multiple bond, and instead, the α-carbon atom receives additional electron density.

Enamines, exploited originally by Stork and co-workers in Stork-enamine alkylations, exhibit an analogous bonding interaction.[38−40] The practicality of enamine chemistry now extends well beyond stoichiometric reactions to exciting discoveries in organocatalysis.[41−45] A simple resonance structure depiction helps to explain the observed increased nucleophilicity of the β-carbon of an enamine (Scheme 1)[39,40]

Scheme 1. Two Possible Resonance Contributions for an Enamine (Top) and Amidoalkylidene (Bottom)

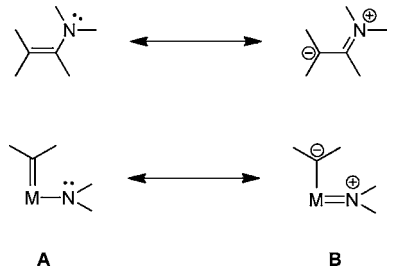

and, therefore, the potential application to metal−carbon multiple bonds. For both examples, the lone pair on nitrogen "pushes" electron density on the carbon atom two bonds away. A somewhat more sophisticated description, albeit perhaps less convincing, involves a delocalization of the N-atom lone pair into the C═C, or in the case of alkylidenes, into the M═C bond (Figure 2). The energetic consequence is the HOMO

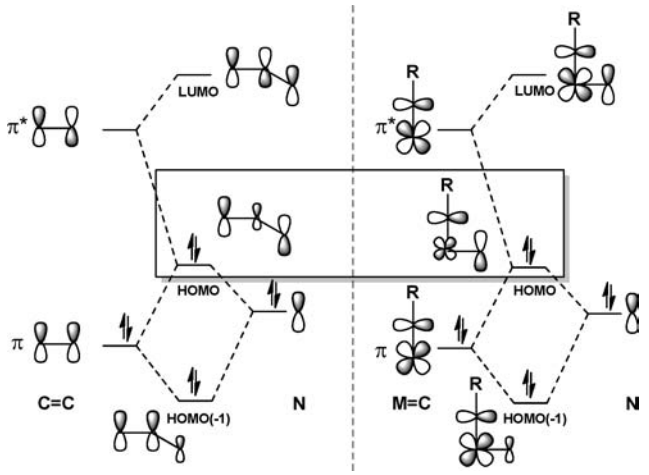

Figure 2. Truncated qualitative orbital diagram of the bonding analogy between enamines[40] and amidoalkylidenes.

orbital, consisting of significant electron density on the β-carbon of the enamine or the α-carbon of an alkylidene, is *destabilized*. The challenge for synthesizing an inorganic version of an enamine is that unrestricted amido ligands preferentially orient the lone pair perpendicular to the M−C bond to maximize bonding with an unoccupied, often d_{xy}, orbital (Figure 1). A solution is to constrain the amido donor in a multidentate ligand. Trianionic NCN[46,47] and OCO[48−51] pincer ligands provide such a rigid meridional environment and have recently been exploited for catalytic aerobic oxidation,[52] alkene isomerization[53] and polymerization,[54,55] alkyne polymerization,[56] and fundamental transformations[57] involving oxygen-atom transfer,[58] nitrogen-atom transfer,[59] and dioxygen activation.[60] In addition, Heyduk et al. introduced redox active trianionic ONO^{3-} and NNN^{3-} pincer-type ligands.[61−64] Yet to be reported is an ONO^{3-} pincer-type ligand that incorporates a push−pull design and is redox insulated.

Figure 3 depicts a new CF_3−ONO^{3-} pincer-type ligand that incorporates all the design features required to create high

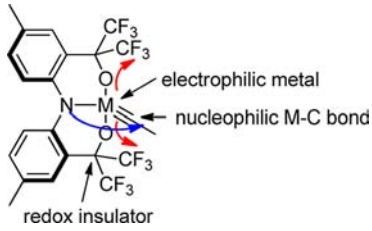

Figure 3. Push−pull effect of the $[CF_3$−$ONO]^{3-}$ pincer-type ligand.

oxidation state nucleophilic metal−carbon multiple bonds. In contrast to Heyduk's ONO^{3-} amido-bisphenoxide ligand,[61,64] which can easily access multiple redox states, the quaternary carbon of the alkoxide acts as a redox insulator. The fluorinated alkoxides induce an electrophilic metal center (pull) and the constrained pincer framework prevents amido π-donation into the d_{xy} orbital, and instead, the lone pair interacts with the metal−carbon bond (push). Accomplishing this objective, we now report the two-step synthesis of the new trianionic pincer-type ligand $[CF_3$−$ONO]H_3$ (**1**) and its corresponding tungsten−alkylidene $[CF_3$−$ONO]W{=}C(Et)(O^tBu)$ (**2**) and −alkylidyne $\{MePPh_3\}\{[CF_3$−$ONO]W{\equiv}C(Et)(O^tBu)\}$ (**3**) complexes. Demonstrating high nucleophilicity, addition of a Me_3SiOTf to **3** expels isobutylene in an intramolecular C−H bond activation pathway. Moreover, the reaction is catalytic for **2**.

RESULTS

Synthesis and Characterization of $[CF_3$−$ONO]H_3$ (1). Preparing the ligand precursor $[CF_3$−$ONO]H_3$ (**1**) involves treating bis(2-bromo-4-methylphenyl)amine[65] with 3.1 equiv of ^{n}BuLi in Et_2O and then adding hexafluoroacetone at −78 °C (eq 1). Warming to 25 °C and an acidic workup yields isolable

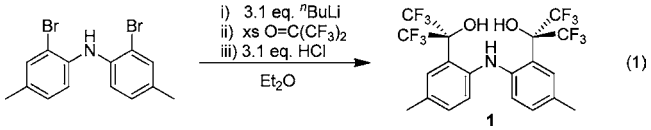

proligand **1** in 35% yield. In the $^{19}F\{^1H\}$ NMR spectrum of **1** ($CDCl_3$), two broad multiplets attributable to the fluorine atoms appear at −76.3 and −74.9 ppm. The fact that two signals appear indicates a slow rotation around the aryl−$C(CF_3)_2OH$ bond at 25 °C. Coalescence of the signals occurs upon heating a sample of **1** to 45 °C in an NMR probe. Routine ^1H and $^{13}C\{^1H\}$ NMR spectroscopic techniques corroborate the identity and purity of **1** (see Supporting Information). Notable features in the ^1H NMR spectrum include a singlet at 2.36 ppm for the aryl−methyl protons and a broad resonance spanning from 7.0 to 7.5 ppm that corresponds to the protons of the amine and the two alcohol groups.

dx.doi.org/10.1021/ja302222s | J. Am. Chem. Soc. 2012, 134, 11185−11195

Synthesis and Characterization of [CF_3−ONO]W═CH(Et)(O^tBu) (2). In benzene, combining proligand **1** with (^{t}BuO)$_3$W≡C(Et)[66] results in the immediate formation of the trianionic pincer alkylidene complex [CF_3−ONO]W═CH-(Et)(O^tBu) (**2**) according to eq 2. Isolation of reasonably pure

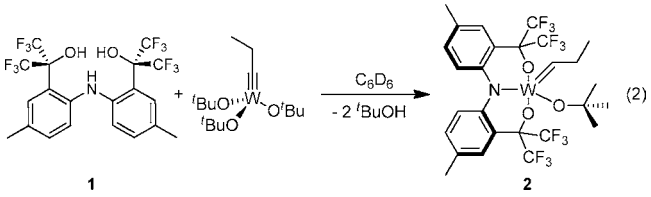

2 only requires removal of all volatiles in vacuo; recrystallizing **2** in pentane provides analytically pure material. Single crystals amenable to an X-ray diffraction experiment deposit upon cooling a concentrated pentane solution of **2** to −35 °C. Structure refinement of the diffraction data provides the molecular structure of **2** presented in Figure 4.

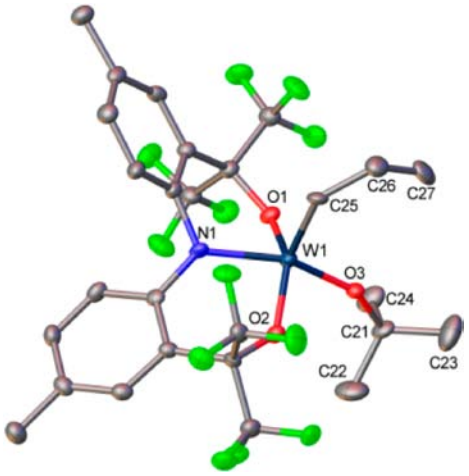

Figure 4. Molecular structure of [CF_3−ONO]W═CH(Et)(O^tBu) (**2**) with ellipsoids drawn at the 50% probability level, with hydrogen atoms removed for clarity.

Complex **2** is C_1-symmetric, and occupying the basal plane of the distorted square-pyramidal tungsten(VI) geometry are the ONO^{3-} trianionic pincer ligand and *tert*-butoxide. In the apical position resides a propylidene ligand with a W−C_α bond length of 1.882(4) Å, which is consistent with a double bond and similar to two other OCO^{3-} trianionic pincer W-alkylidenes that have bond lengths of 1.887 and 1.913 Å.[67] Consistent with a W═C double bond, the $^{13}C\{^1H\}$ NMR spectrum of **2** contains a downfield resonance at 260.3 ppm [$^1J(^{13}C,^{183}W)$ = 173.1 Hz] and the corresponding alkylidene proton (W═C*H*R) resonates as a triplet at 7.36 ppm. An interesting structural feature appears in the trianionic pincer ligand framework. Unable to lie coplanar, the N-aryl rings twist, thereby lowering the solid-state symmetry from potentially C_s to C_1. This twist and resulting low symmetry persists in solution as four distinct quartets appear in the $^{19}F\{^1H\}$ NMR spectrum of **2** at −71.2, −71.5, −73.9, and −77.2 ppm. The low symmetry also results in diastereotopic −C$_\beta$H$_2$− methylene protons for the propylidene ligand that appear as two multiplets at 5.08 and 4.79 ppm. The propylidene methyl appears as a triplet at 0.77 ppm (^3J = 7.36 Hz). The nitrogen atom of the ONO ligand is trigonal planar [sum of angles = 359.6(4)], consistent with sp^2 hybridization.

The alkylidene bond orients with the alkyl group pointing away from the amido (anti-isomer) and does not rotate with an appreciable rate even at 100 °C. No signals attributable to an exchange with the syn-isomer appear in variable temperature ^1H NMR spectra of **2** from −60 to 100 °C. In Schrock's tungsten imido alkylidene, the syn-isomer predominantly forms ($K_{syn/anti}$ = 5000), but access to the anti-isomer is possible by exposing a sample to UV-radiation at −85 °C for several hours.[68] The relaxation of the anti-isomer back to syn occurs between −53 and −38 °C.[68] Interestingly, the rate of relaxation decreases as the alkoxide ligands become more fluorinated.[69] Invoking similar conditions for complex **2**, a toluene-d_8 solution of **2** exposed to 366 nm light for 4 h at −78 °C does not yield any detectable syn-isomer, as determined by ^1H NMR (500 MHz) spectroscopy.

Synthesis and Characterization of {[CF_3−ONO]W≡C(Et)(O^tBu)}{$MePPh_3$} (3). Deprotonating alkylidenes with methylenetriphenylphosphorane (Ph_3P═CH_2) is a convenient method to access the corresponding alkylidyne anion.[70] Treating alkylidene **2** with Ph_3P═CH_2 in pentane at 25 °C precipitates the W-alkylidyne anion **3** (eq 3). Complex **3** turns

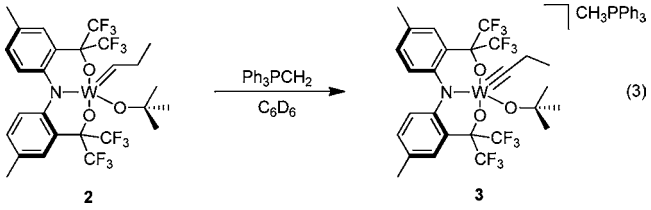

to a bright red color upon dissolving in benzene or ether. Removing the solvent by vacuum yields a red oil, but the addition of cold pentane returns **3** to a yellow powder.

Multinuclear ^1H−^{13}C gHSQC and ^1H−^{13}C gHMBC NMR spectroscopic experiments confirm the identity of **3** and permit the absolute assignment of all resonances in the ^1H and $^{13}C\{^1H\}$ NMR spectra (see Supporting Information). Most pronounced is the downfield shift to 280.6 ppm for the W≡C_α alkylidyne carbon in the $^{13}C\{^1H\}$ NMR spectrum. In the ^1H NMR spectrum, a doublet (J_{HP} = 13.31 Hz) at 2.44 ppm is attributable to the methyl protons of the phosphonium countercation, and the corresponding phosphorus resonates at 21.8 ppm in the $^{31}P\{^1H\}$ NMR spectrum. Consistent again with a C_1-symmetric complex, the ^{19}F NMR spectrum contains four distinct quartets at −69.38, −71.24, −74.08, and −76.38 ppm.

Reactivity Studies, Nucleophilic at Carbon. Adding methyl triflate to **3** in a sealable NMR tube results in alkylation of the alkylidyne carbon to form [CF_3−ONO]W═C(Me)-(Et)(O^tBu) (**4**) (eq 4). Confirming the identity of **4**, a ^1H

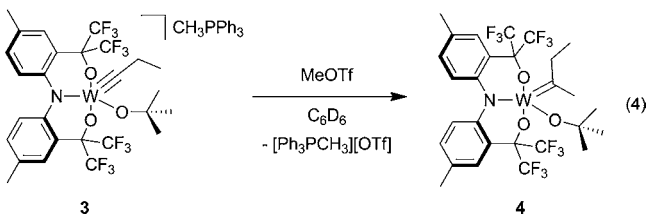

NMR spectrum of the reaction mixture reveals a resonance attributable to the newly formed methyl protons (W═C(C*H*$_3$)Et) at 4.90 ppm (3H). The −C$_\beta$H$_2$− methylene protons are diastereotopic, resonating as two sets of multiplets

dx.doi.org/10.1021/ja302222s | J. Am. Chem. Soc. 2012, 134, 11185−11195

at 4.65 and 4.53 ppm, similar to complex **2**. The $-O^tBu$ protons resonate at 1.21 ppm (9H). The $W-C_\alpha$ resonates at 284.3 ppm, consistent with other reported tungsten dialkyl-substituted alkylidenes.[71−73] The $^1H-^{13}C$ gHMBC spectrum of **4** confirms the connectivity among the methyl protons at 4.90 ppm, the diastereotopic methylene protons at 4.65 and 4.53 ppm, and the alkylidene carbon. Unidentifiable and inseparable minor impurities precluded the large-scale purification of **4**.

Isobutylene Expulsion from 3. Adding the larger electrophile Me_3SiOTf to complex **3** in a sealable NMR tube provides an interesting result. The products observed by ^1H NMR spectroscopy are isobutylene (4.71 ppm, 2H; and 1.56 ppm, 6 H) and the new alkylidene complex $[CF_3-ONO]W{=}CH(Et)OSiMe_3$ (**5**). Complex **5** exhibits a new set of diastereotopic $-C_\beta H_2-$ methylene protons at 5.28 and 4.91 ppm, and the trimethylsiloxide protons appear at 0.12 ppm. Corroborating the identity of **5**, the W=C*H* proton resonates at 7.20 ppm and the corresponding $^{13}C\{^1H\}$ signal appears at 262.1 ppm. Multinuclear $^1H-^{13}C$ gHSQC and $^1H-^{13}C$ gHMBC NMR spectroscopic experiments confirm the identity of **5** and permit the absolute assignment of all resonances in the ^1H and $^{13}C\{^1H\}$ NMR spectra (see Supporting Information). Complex **5** is unstable at ambient temperature and decomposes to unidentifiable and intractable impurities.

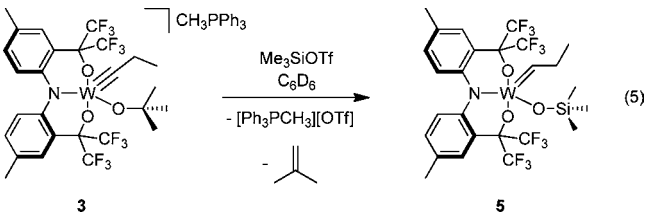

Catalytic Isobutylene Expulsion from 2. As mentioned above, complex **2** contains a restricted amide rotation similar to that of complex **3**. The amide lone pair and alkylidene of **2** form a torsion angle of 44.34°, potentially creating a nucleophilic M=C *double* bond.

Indeed, treating complex **2** with Me_3SiOTf also results in isobutylene expulsion as well as the formation of $[CF_3-ONO]W(O)^nPr$ (**6**). The absence of Me_3SiOTf in the product suggests it acts as a catalyst in the expulsion of isobutylene from **2**. Indeed, adding 5 mol % Me_3SiOTf, MeOTf, or $B(C_6F_5)_3$ to a solution of **2** catalyzes isobutylene expulsion to form **6** quantitatively by ^1H NMR spectroscopy (eq 6). Stripping the

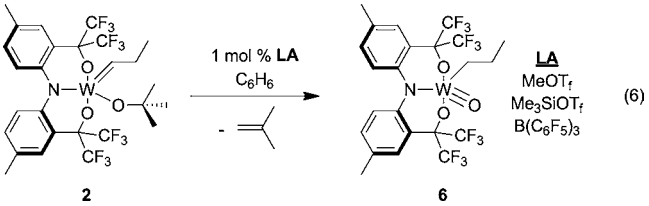

solvent from **6** initially yields a thick blue oil, but crystals suitable for single crystal X-ray analysis gradually form (isolated yield = 73%). The solid state structure of **6** (Figure 5) contains a tungsten(VI) ion in a trigonal bipyramidal geometry with equatorial plane angles N1−W1−O3 = 129.69°, N1−W1−C21 = 121.46°, and C21−W1−O3 = 108.82(10)°. The W1−O3 bond is 1.704 Å, which is consistent with other reported neutral $W^{VI}{\equiv}O$ complexes.[74−93] The $^{19}F\{^1H\}$ NMR of **6** confirms a C_1 symmetric species in solution with four quartets at −71.2, −71.8, −75.6, and −76.4 ppm. The α-protons of the propyl group $\{WCH_2CH_2CH_3\}$ resonate in the ^1H NMR spectrum as a multiplet at 3.00 ppm. The β-protons and γ-protons of the propyl group appear as a multiplet at 2.65 ppm and a triplet at 0.92 ppm, respectively. The nitrogen atom is sp^2 hybridized and a vector perpendicular to the amido plane, representing the lone pair on nitrogen, forms a 39.72° torsion angle with the W≡O bond.

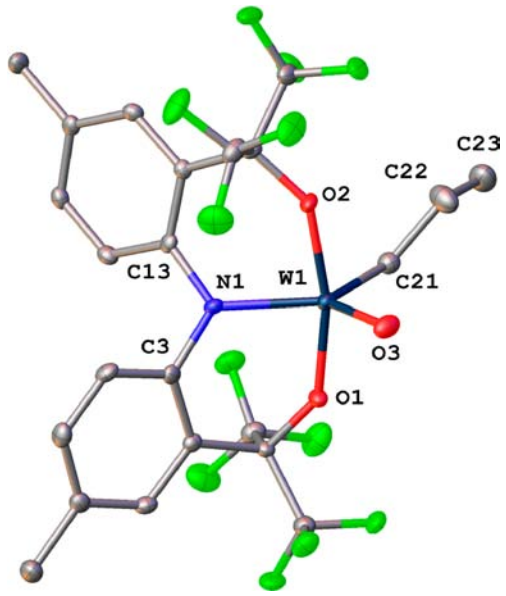

Figure 5. Molecular structure of $[CF_3-ONO]W(O)\ ^nPr$ (**6**) with ellipsoids drawn at the 50% probability level, with hydrogen atoms removed for clarity.

COMPUTATIONAL RESULTS

Employing DFT calculations, the model complexes **2′**, **2-Me′**, and **3′**, representing **2**, the intermediate **2-Me**, and **3**, respectively, were geometry optimized. Figure 6 depicts the computed structures and Table 1 lists pertinent bond lengths and angles. Experimental bond lengths and angles for **2** serve to calibrate the calculated structure of **2′**. The tungsten coordination sphere metric parameters are agreeable and it is clear that the calculation reproduces the twist of the ONO backbone observed experimentally. A vector perpendicular to the C3−W1−C13 plane, representing the nitrogen lone pair, creates a 41.7° dihedral angle with the W1−C1 bond axis (the experimental value is 40.5°). Also, the alkylidene orients in the same direction as in **2**. The alkylidene ethyl group points away from the N-atom. A quantifiable parameter confirming the similar orientation is the dihedral angle C22−C21−W1−O3; for **2** it is 10.2° and within **2′** it is 11.7°. In general, there is a small overestimate of most of the bond lengths by 0.02 Å or less. For example, the N1−W1 distance of 2.013 Å in **2′** is slightly longer than in **2** [1.993(3) Å], and the computed alkylidene W1−C21 bond length of 1.898 Å matches the experimental value of 1.882(4) Å.

The computed structures of **2-Me′** and **3′** also reproduce the ONO twist and some interesting trends emerge between the set of three complexes. Most apparent is the W−N bond distance, which increases with **2-Me′** (1.982 Å) < **2′** (2.013 Å) < **3′** (2.142 Å). The computation accurately predicts a trend assignable to an increase in electronic saturation at the metal ion. Complex **3′** is anionic, thus electron-rich, whereas **2-Me′** is

dx.doi.org/10.1021/ja302222s | J. Am. Chem. Soc. 2012, 134, 11185−11195

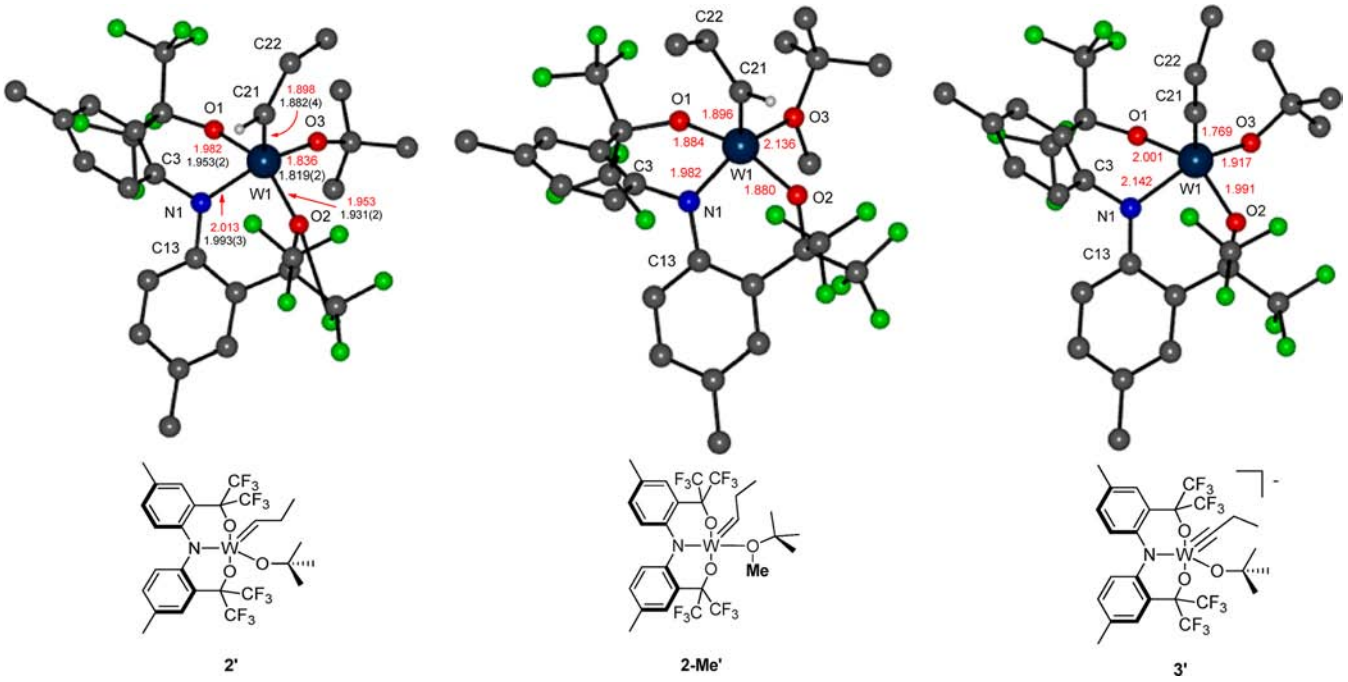

Figure 6. Geometry-optimized structures for **2′**, **2-Me′**, and **3′**.

Table 1. Selected Bond Lengths (Å) and Angles (deg) for the Single Crystal X-ray Structure of 2 and DFT Geometry-Optimized Structures of 2′, 2-Me′, and 3′

bond lengths	2	2′	2-Me′	3′
W1−O1	1.953(2)	1.982	1.884	2.001
W1−O2	1.931(2)	1.953	1.880	1.991
W1−O3	1.819(2)	1.836	2.136	1.917
W1−N1	1.993(3)	2.013	1.982	2.142
W1−C21	1.882(4)	1.898	1.986	1.769
C21−C22	1.499(5)	1.519	1.507	1.493
O3−C28			1.498	
angles	**2**	**2′**	**2-Me′**	**3′**
O1−W1−O2	144.95(11)	145.68	156.17	146.18
O1−W1−C21	104.44(13)	103.65	99.44	103.39
N1−W1−O3	154.64(11)	155.42	151.23	153.28
N1−W1−C21	99.81(14)	97.98	101.36	98.06
O2−W1−C21	109.41(13)	108.38	104.08	106.26
O3−W1−C21	105.50(13)	106.48	107.40	108.65
C22−C21−W1	137.2(3)	137.44	134.18	176.20
C28−O3−W1				111.50

electron-poor, due to the loss of π-donation upon methylating the alkoxide O-atom. Correspondingly, the W−O bond length of 2.136 Å for the bound *tert*-butyl methyl ether in **2-Me′** is appropriately longer than the *tert*-butoxide of **3′**, and only slight shorter by ∼0.05 Å than the crystallographically characterized diethyl ether W−O bond of 2.185(2) Å found in the related OCO^{3-} pincer alkylidyne [^{t}BuOCO]W≡C(^{t}Bu)(Et_2O).[56]

The most salient feature of complex **3′** is the alkylidyne W≡C bond with a length of 1.769 Å that matches experimentally determined values. Though there are no structurally characterized trianionic pincer alkylidyne anions known, two neutral OCO^{3-} pincer complexes have W≡C bond lengths of 1.755(2) and 1.759(4) Å. For additional comparison, Schrock's $(ArO)_2$NpW≡C(^{t}Bu)[94] complex contains a W≡C bond length of 1.755(2) Å, a difference of only ∼0.01 Å with that of **3′**. Considering the reasonable match in metric parameters, single point calculations of each complex were performed and the resulting electronic structures were evaluated (vide infra).

DISCUSSION

MeOTf alkylation at the C_α atom of the alkylidyne in **3** has a different reactivity pattern compared to previous examples. Alkylating agents preferentially attack the ancillary ligands, leaving both neutral and anionic tungsten alkylidynes intact.[95] Similarly for anionic molybdenum imido alkylidyne complexes, both small ([Me_3O][BF_4]) and large (Me_3SiOTf) electrophiles selectively attack the imido N-atom.[70] The direct alkylation of the W≡C_α bond by MeOTf has no precedent in the literature. Enamines react with electrophiles at the β-position, whereas unfuctionalized alkenes do not. Electronically, complex **3** is analogous to an enamine. Examining the electronic structure of **3** through single-point calculations provides insight into how the CF_3−ONO pincer ligand influences the tungsten alkylidyne bond.

Figure 7 (left) depicts a truncated molecular orbital diagram that illustrates the bonding combination between the amido lone pair and the W≡C π-bond. The key feature is the forced torsion angle between the alkylidyne bond and the amide lone pair. This contrasts the typical arrangement in which the nitrogen lone pair orients perpendicularly to the alkylidyne bond to maximize π-donation into the empty d_{xy}. The rigid ONO pincer geometry within **3** prevents the amide from orienting perpendicularly to the alkylidyne and instead the LUMO of **3′**, consisting of the d_{xy} orbital, contains no orbital interaction with the amido lone pair (Figure 7, left).

The alkylidyne π-bond facing the nitrogen [HOMO(−2)] displays overlap with the nitrogen's lone pair, lowering its energy relative to the adjacent π-bond [HOMO(−1)] by 0.01139 au (Figure 7, left). A torsion angle of 42.8° between the lone pair and the alkylidyne bond results in significant overlap. The corresponding antibonding combination corresponds to the HOMO orbital analogous to an enamine (Figure

dx.doi.org/10.1021/ja302222s | J. Am. Chem. Soc. 2012, 134, 11185−11195

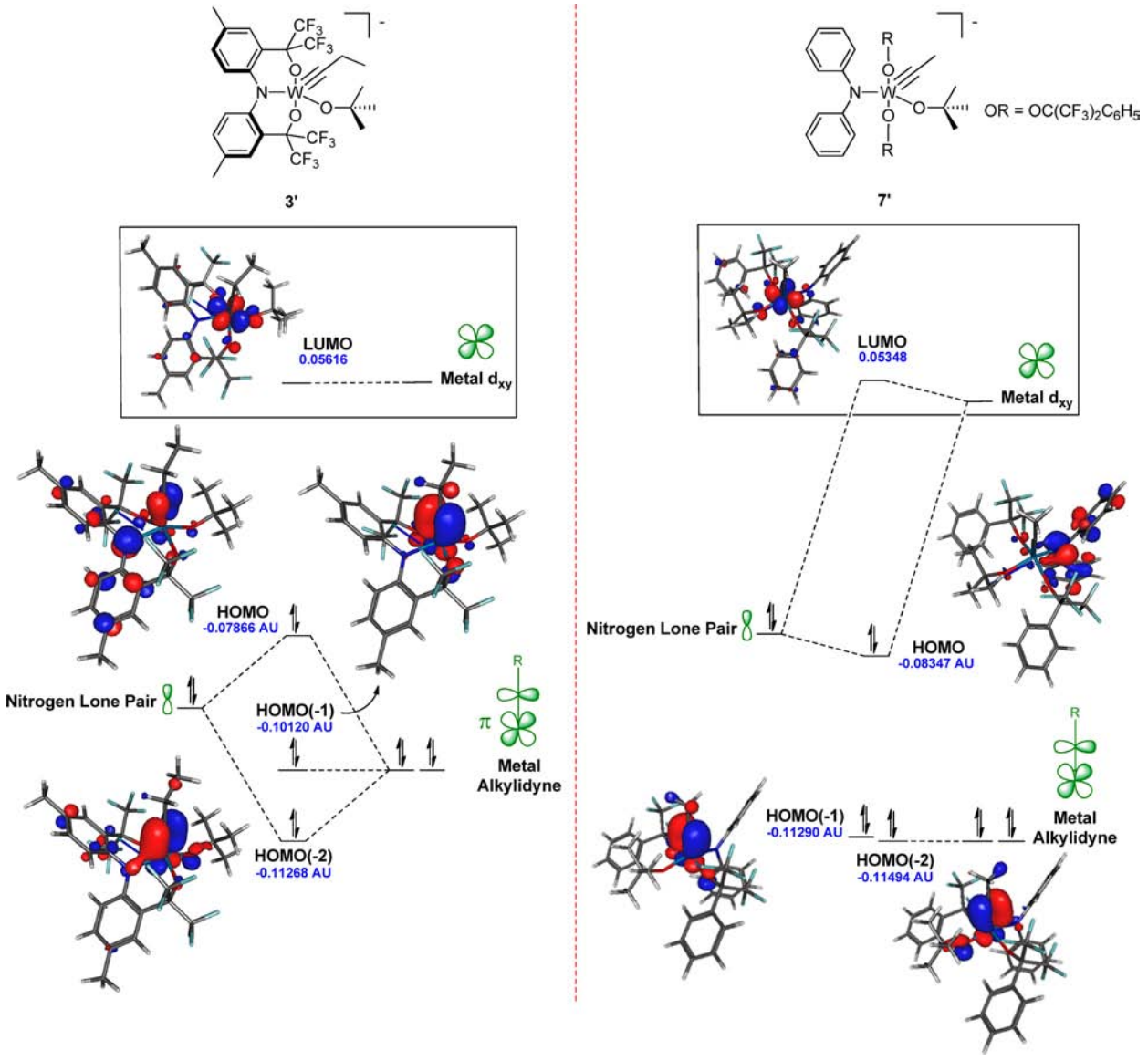

Figure 7. (Left) The HOMO, HOMO(−1), and HOMO(−2) orbitals of **3′**. (Right) The HOMO, HOMO(−1), and HOMO(−2) orbitals of **7′** (isovalue = 0.051 687).

2). This bonding−antibonding interaction raises the energy of the HOMO, thus increasing the nucleophilicity of the alkylidyne α-carbon.

In stark contrast is the single-point calculation from a geometry-optimized structure performed on the model anionic alkylidyne $\{(Ph_2N)W{\equiv}C(Me)(OC(CF_3)_2Ph)_2(O^tBu)\}^-$ (**7′**). The amido ligand orientation matches the analogous complex $\{3,5\text{-}C_6H_3Me_2)^tBuN\}W{\equiv}C(^tBu)\{OC(CF_3)_2Me\}_2$ calculated by Tamm and co-workers.[31] Depicted in Figure 7 (right) are the single point calculations of **3′** and **7′**, aligned for easy comparison. The model complex **7′** features an unrestricted amido ligand $N(C_6H_5)_2$, yet retains the electron-withdrawing $OC(CF_3)_2C_6H_5$ groups. In **7′** the amido ligand orients to maximize π-donation into the empty d_{xy} orbital, which serves to stabilize the HOMO orbital comprised mostly of the N-atom lone pair. However, the M−C π-bonding orbitals are completely unaffected by the N-atom lone pair. By comparing the electronic structures, it is evident that purposely constraining the N-atom lone pair to be collinear with the M≡C bond destabilizes the HOMO orbital and places increased electron density on the α-carbon.

Isobutylene expulsion provides more evidence for the nucleophilicity of **3**. Scheme 2 illustrates a proposed mechanism for isobutylene expulsion. In the first step, Me_3SiOTf attacks the *tert*-butoxide ligand to yield the trimethylsilyl-*tert*-butyl ether adduct, **3-SiMe$_3$**. Then, acting as a nucleophile, the W-alkylidyne deprotonates the *tert*-butyl group to expel isobutylene and form **5**. *tert*-Butoxide is a common ligand, especially for tungsten complexes featuring M−C multiple bonds, but this is the first occurrence of its degradation via alkylidyne deprotonation and is clear evidence of the highly nucleophilic character of the W−C_α atom.

Additional evidence that the N-atom plays an important role comes from reactivity studies employing the related OCO^{3-} pincer ligand. Without the N-atom a different reaction occurs; addition of MeOTf to the analogous OCO trianionic pincer alkylidyne anion $\{MePPh_3\}\{[^tBuOCO]W{\equiv}C(^tBu)(O^tBu)\}$ produces $[^tBuOCO]W{\equiv}C(^tBu)(OEt_2)$.[56] The reaction proceeds via Me-alkylation of the *tert*-butoxide *but deprotonation*

dx.doi.org/10.1021/ja302222s | J. Am. Chem. Soc. 2012, 134, 11185−11195

Scheme 2. Proposed Mechanism for Isobutylene Expulsion from 3

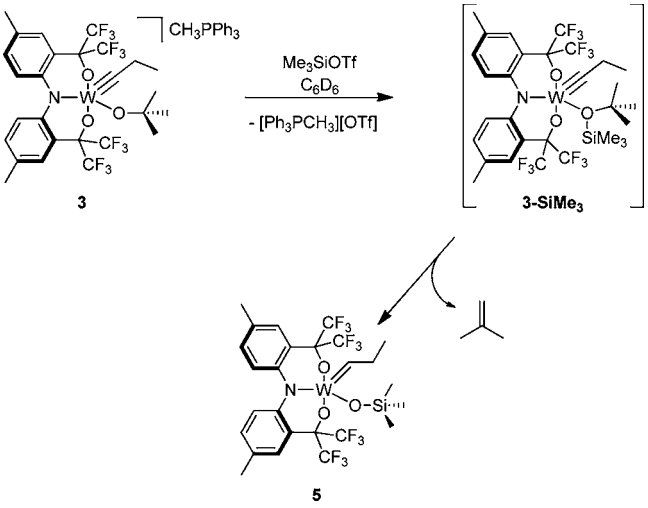

Scheme 3. Proposed Mechanism for Isobutylene Expulsion from 2 (LA = Me^+, Me_3Si^+, and $B(C_6F_5)_3$

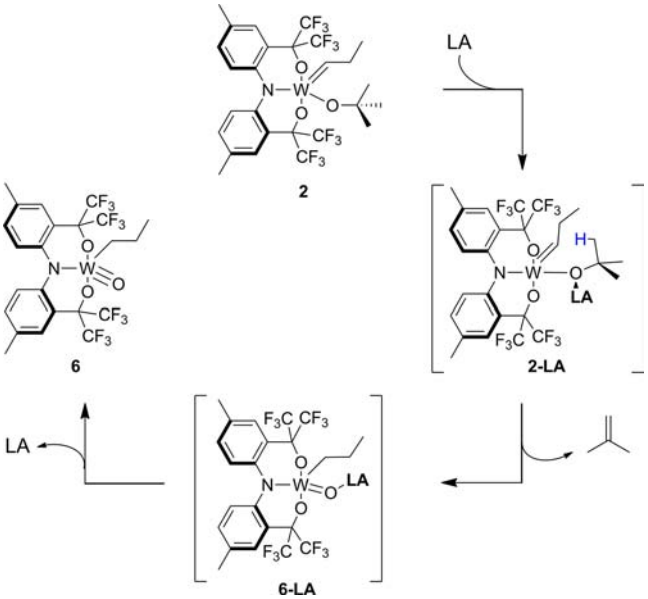

does not occur; instead, MeO^{t}Bu forms. Notably, the Me^+ adds to the alkoxide and not the alkylidyne α-carbon as in **3**.

Not all of the divergent chemistry between the CF_3−ONO^{3-} and the OCO^{3-} ligands are attributable to the N-atom alone. An additional significant difference is the fluorinated alkoxides on CF_3−ONO^{3-}, which create an electrophilic tungsten ion. Silylating the −O^{t}Bu of **3** removes π-donation from the alkoxide and leaves only a weakly σ-donating ether. The result is an even more electrophilic tungsten metal. Yet, other electrophilic tungsten alkylidynes supported by three −OC(CF$_3$)Me are known metathesis catalysts that show stability toward substrates containing ether, ester, ketone, aldehyde, acetal, and thioether moieties[96] and are only protonated via hydrohalic acids.[97,98] The combination of the N-atom and the electron-withdrawing CF_3 groups must lead to deprotonation of the *tert*-butoxide.

The Lewis acid-catalyzed expulsion of isobutylene from **2** demonstrates that W−C double bonds with the CF_3−ONO^{3-} ligands are also highly nucleophilic. Scheme 3 depicts the proposed mechanism for the Lewis acid-catalyzed isobutylene expulsion from **2**. Two plausible sites for electrophilic (**LA**) attack on **2** are the amido N-atom and the *tert*-butoxide O-atom. The N-atom is too sterically crowded, especially for large electrophiles such as $B(C_6F_5)_3$ and Me_3SiOTf, which catalyze the reaction too. Thus, initial attack must occur at the *tert*-butoxide to form **2-LA**. Proceeding from **2-LA**, the alkylidene deprotonates the ^{t}Bu group to form isobutylene and **6-LA**. The Lewis acid catalyst is then released to provide **6**.

An interesting question arises regarding the deprotonation event. Structural characterization and subsequent variable-

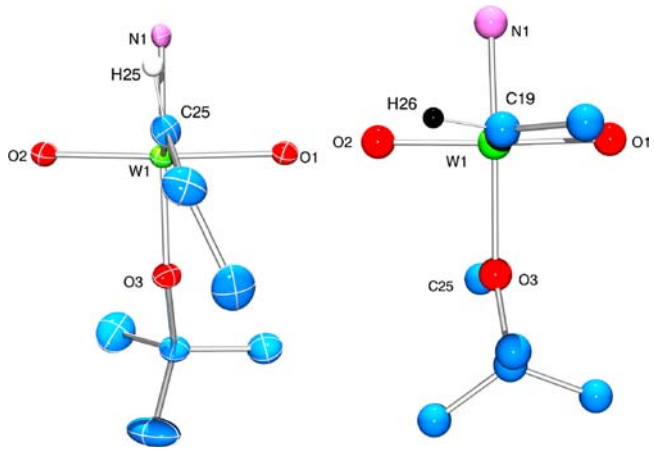

Figure 8. Truncated X-ray structure of **2** (left) and geometry-optimized structure **2-Me′** (right) illustrating the 77° rotation of the W=C bond.

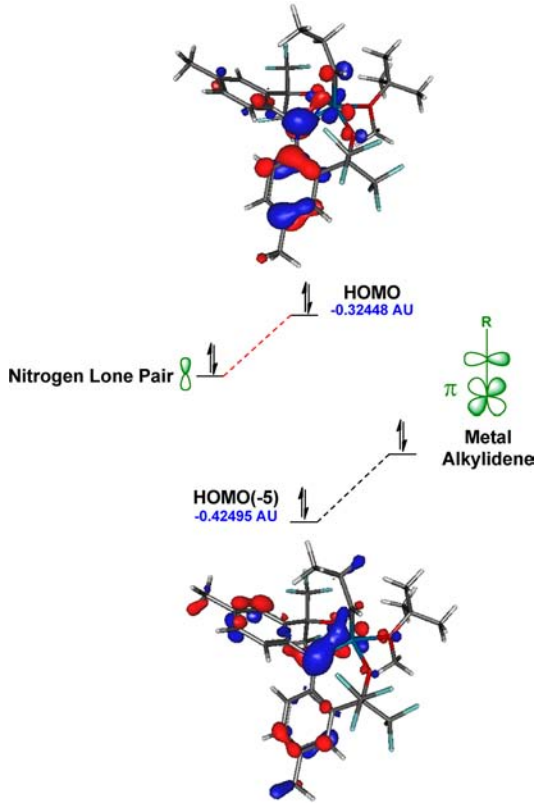

Figure 9. The HOMO, HOMO(−1), and HOMO(−5) orbitals of **2-Me′** (isovalue = 0.051 687).

dx.doi.org/10.1021/ja302222s | J. Am. Chem. Soc. 2012, 134, 11185−11195

temperature NMR experiments indicate that the alkylidene W=C bond in **2** is perpendicular to the *tert*-butoxide ligand (see Figure 8 for an illustration). To complete the deprotonation the π-bond needs to approach the proton of the *tert*-butoxide. Curious as to the orientation of the alkylidene in **2-LA**, we performed a geometry optimization calculation of **2-Me′**, in which Me^+ serves as the Lewis acid (see Figure 6 above). The electrophile accepts a pair of electrons from the oxygen atom that normally π-donate into the W-d_{xy} orbital. Most pronounced and interestingly, the alkylidene in **2-Me′** rotates ~77° from that of the experimentally determined structure of **2**. Illustrated in Figure 8 is a truncated X-ray structure of **2** and the computed structure **2-Me′**. The double bond clearly orients toward the MeO^{t}Bu. A single-point calculation of **2-Me′** again reveals that the HOMO and HOMO(−5) are the amide/alkylidene π-antibonding and π-bonding orbitals, respectively, analogous to that calculated for **3** and a prototypical enamine (Figure 9). The LUMO of **2-Me′** (not depicted) consists of the d_{xy} orbital and contains only a small component from the N-atom lone pair and ether ligand.

CONCLUSION

Presented above is evidence for an inorganic enamine: a unique strategy for creating nucleophilic W−C multiple bonds by constraining an amide ligand lone pair orientation. Traditionally, tungsten alkylidenes/alkylidynes are weakly nucleophilic. Thus, a straightforward synthetic strategy to create nucleophilic alkylidene and alkylidyne complexes is to purposely orient an amido ligand lone pair toward the alkylidyne/alkylidene bond. To accomplish this feat we report the convenient two-step synthesis of a new CF_3−ONO^{3-} trianionic pincer-type ligand. The "push" via alignment of an amido lone pair, coupled to the "pull" of the CF_3 groups, serve to polarize the M−C bond and create a nucleophilic α-carbon. Evidence is the direct alkylation of the alkylidyne in **3** with MeOTf; and isobutylene expulsion upon addition of the larger Me_3SiOTf. Complementing these results is the Lewis acid-catalyzed expulsion of isobutylene from **2**, proposed to occur via *tert*-butyl deprotonation by the nucleophilic α-carbon of the W=C bond. The reaction works with several Lewis acids [MeOTf, Me_3SiOTf, and $B(C_6F_5)_3$] and insight into their role comes from a geometry optimization of the proposed Lewis acid adduct **2-Me′**. The calculation reveals a critical reorientation of the alkylidene double bond that places it according to an enamine alignment and in position to deprotonate the *tert*-butyl group.

Using a trianionic pincer framework to constrain amide orientation provides a new approach to increasing nucleophilicity of M−C multiple bonds. Another example of a constrained amido adjacent to M−C multiple bonds is Mindiola's PNP^{1-} titanium alkylidyne,[12−21] though being a first row metal and already highly nucleophilic, the amide contribution may be difficult to assess. The ease of synthesis of proligand **1** relative to other trianionic pincer ligands will facilitate exploration of this ligand with many other metal ions as well as other M−X multiple bonds (where, X = O, N, and P).

EXPERIMENTAL SECTION

General Procedure. Unless specified otherwise, all manipulations were performed under an inert atmosphere using standard Schlenk or glovebox techniques. Pentane, hexanes, toluene, diethyl ether (Et_2O), dichloromethane, tetrahydrofuran (THF), and 1,2-dimethoxyethane (DME) were dried using a GlassContour drying column. Benzene-d_6 (Cambridge Isotopes) was dried over sodium−benzophenone ketyl, distilled or vacuum transferred, and stored over 4 Å molecular sieves. Bis(2-bromo-4-methylphenyl)amine,[65] PPh_3CH_2,[70] and (^{t}BuO)$_3$W≡C(Et)[66] were prepared according to published literature procedures. All other reagents were purchased from commercial vendors and used without further purification. NMR spectra were obtained on Varian Gemini 300 MHz, Varian Mercury Broad Band 300 MHz, or Varian Mercury 300 MHz spectrometers. Chemical shifts are reported in δ (ppm). For ^{1}H and $^{13}C\{^1H\}$ NMR spectra, the solvent peak was referenced as an internal reference. Infrared spectra were obtained on a Thermo Scientific Nicolet 6700 FT-IR.

DFT Calculations. Spin-restricted density functional theory calculations, including geometry optimization and single point analysis, were performed for **2′**, **2-Me′**, **3′**, and **7′** using a hybrid functional (the three parameter exchange functional of Becke (B3)[99] and the correlation functional of Lee, Yang, and Parr (LYP)[100] (B3LYP) as implemented in the Gaussian 03 program suite.[101] The LANL2DZ basis set were used for all atoms within **2′**, **2-Me′**, **3′**, and **7′**.[102] The geometry was optimized using atomic coordinates from the crystal structure as an initial input and calculations for the vibrational frequencies were performed alongside the geometry optimization to ensure the stability of the ground state as denoted by the absence of imaginary frequencies. Molecular orbital pictures were generated from Gabedit at their reported isovalues.

Synthesis of 2,2′-(Azanediylbis(3-methyl-6,1-phenylene))-bis(1,1,1,3,3,3-hexafluoropropan-2-ol) (1). Inside a nitrogen-filled glovebox, an *n*-butyllithium solution (10.9 mL, 2.5 M, 27.3 mmol) was added dropwise to a Schlenk-flask containing a solution of bis(2-bromo-4-methylphenyl)amine (3.103 g, 8.79 mmol) in diethyl ether (30 mL) at −35 °C. The reaction mixture was stirred for 2 h while warming to room temperature. The reaction flask was fitted with a dry ice condenser before exiting the box. The reaction flask was connected to a Schlenk line through the port on the dry ice condenser. The reaction solution was cooled to −78 °C, and dry ice and acetone were added to the condenser. Hexafluoroacetone was first measured into a graduated glass pressure flask by condensing at −78 °C (5 mL, 6.6 g, 39 mmol). The pressure flask was then connected to the reaction flask via a side arm. The pressure flask was allowed to slowly warm to room temperature, causing the hexafluoroacetone to evaporate and condense into the reaction flask. After complete transfer, the pressure flask was removed. The reaction mixture was allowed to warm to room temperature while the dry ice/acetone condenser was kept filled (the hexafluoroacetone will condense on the coldfinger and drip back into the solution). The reaction mixture was stirred for at least 3 h before allowing the dry ice/acetone to expire and the excess hexafluoroacetone to leave through the Schlenk manifold. To the resulting red solution was added HCl in Et_2O (27.3 mL, 1 M). A colorless precipitate formed (LiCl) and the mixture was filtered. The filtrate was reduced under vacuum to a thick oil followed by adding hexanes to precipitate the product as a light-pink powder, which was filtered (1.66 g, 35% yield). ^{1}H NMR ($CDCl_3$, 300 MHz, 25 °C): δ = 7.5−7.0 (b, 3 H, N*H* and 2 O*H*), 7.37 (s, 2H, Ar-*H*), 7.17 (d, 2H, ^3J = 8.35 Hz, Ar-*H*), 8.83 (d, 2H, ^3J = 8.35 Hz, Ar-*H*), and 2.36 (s, 3H, C*H*$_3$) ppm. $^{19}F\{^1H\}$ NMR ($CDCl_3$, 282 MHz, 25 °C): δ = −74.9 (b) and −76.3 (b) ppm. $^{13}C\{^1H\}$ NMR ($CDCl_3$, 75 MHz, 25 °C): δ = 142.8 (s, Ar *C*), 134.3 (s, Ar *C*), 132.1 (s, Ar *C*), 128.5 (s, Ar *C*), 126.0 (s, Ar *C*), 120.78 9 (s, Ar *C*), and 21.0 (s, *C*H$_3$) ppm. $^{13}C\{^{19}F\}$ NMR ($CDCl_3$): δ = 122.8 (s, CF_3) and 80.3 (s, Ar(CF_3)$_2$*C*OH) ppm. ESI-MS: 530.0984 [1 + H]$^+$, 552.0803 [1 + Na]$^+$, and 574.0623 [1 − H + 2Na]$^+$.

Synthesis of [CF_3−ONO]W=CH(Et)(O^{t}Bu) (2). A benzene solution (2 mL) of **1** (376.4 mg, 0.711 mmol) and W≡C(Et)(O^{t}Bu)$_3$ (315.9 mg, 0.711 mmol) were combined and stirred for 0.5 h. The solvent was evaporated and the residual solid was placed under vacuum for 4 h. Single crystals of **2** were grown from a pentane solution at −35 °C (0.352 g, 60%). ^{1}H NMR (C_6D_6, 300 MHz, 25 °C): δ = 7.72 (s, 2H, Ar-*H*), 7.36 (t, 1H, ^3J = 7.64 Hz, WC*H*CH$_2$CH$_3$), 6.81 (d, 1H, ^3J = 8.49 Hz, Ar-*H*), 6.66 (d, 1H, ^3J = 8.21 Hz, Ar-*H*), 6.60 (d, 1H, ^3J = 9.06 Hz, Ar-*H*), 6.59 (d, 1H, ^3J = 8.49 Hz, Ar-*H*), 5.08 (ddq, 1H, ^2J = 15.0 Hz, ^3J = 7.36 Hz, ^3J = 7.36 Hz, WCHC(H′)(*H*)CH$_3$), 4.79 (ddq, 1H, ^2J = 15.0 Hz, ^3J = 7.36 Hz, ^3J = 7.36 Hz, WCHC(*H*′)(H)CH$_3$), 2.00 (s, 3H, C*H*$_3$′), 1.96 (s, 3H,

dx.doi.org/10.1021/ja302222s | J. Am. Chem. Soc. 2012, 134, 11185−11195

CH_3), 1.21 (s, 9H, $OC(CH_3)_3$, and 0.77 (t, ^3J = 7.36 Hz, $WCHCH_2CH_3$) ppm. $^{19}F\{^1H\}$ NMR (C_6D_6, 282 MHz, 25 °C): δ = −71.2 (q, 3F, ^4J = 9.61 Hz), −71.5 (q, 3F, ^4J = 12.0 Hz), −73.9 (q, 3F, ^4J = 9.60 Hz), and −77.2 (q, 3F, ^4J = 9.61 Hz) ppm. $^{13}C\{^1H\}$ NMR (C_6D_6, 126 MHz, 25 °C): δ = 260.3 (s, $WCHCH_2CH_3$, with satellites $^1J(^{13}C,^{183}W)$ = 173.1 Hz), 146.8 (s, Ar *C*), 145.8 (s, Ar *C*), 135.1 (s, Ar *C*), 134.6 (s, Ar *C*), 133.0 (s, Ar *C*), 131.7 (s, Ar *C*), 127.5 (s, Ar *C*), 124.7 (s, Ar *C*), 124.5 (s, Ar *C*), 124.3 (s, Ar *C*), 90.3 (s, $OCMe_3$), 33.6 (s, $WCHCH_2CH_3$), 29.8 (s, $OC(CH_3)_3$), 21.4 (s, $WCHCH_2CH_3$), 21.0 (s, Ar-CH_3′), and 20.8 (s, Ar-CH_3) ppm. Anal. Calcd for $C_{27}H_{27}F_{12}NO_3W$ (825.33 g/mol): C, 39.29; H, 3.30; N, 1.70. Found: C, 39.25; H, 3.37; N, 1.58.

Synthesis of {[CF_3−ONO]W≡C(Et)(O^tBu)}{$MePPh_3$} (3). A pentane solution of CH_2PPh_3 (131.5 mg, 0.476 mmol, 1.6 equiv) was filtered prior to dropwise addition to a stirring pentane solution of **2** (243.4 mg, 0.295 mmol, 1 equiv). Red oil formed upon complete addition and the reaction mixture was triturated in the pentane solution for 6 h to yield a yellow powder. The powder was filtered, washed with pentane, and dried overnight (0.170 g, 83%). ^1H NMR (C_6D_6, 300 MHz, 25 °C): δ = 7.81 (s, 1H, Ar-*H*), 7.66 (s, 1H, Ar-*H*), 7.51 (d, 1H, Ar-*H*, ^3J = 8.35 Hz), 7.20 (d, 1H, Ar-*H*, ^3J = 8.95 Hz), 7.01 (b, $(C_6H_5)_3PCH_3$), 6.98 (b, $(C_6H_5)_3PCH_3$) 6.92 (dd, 1H, Ar-*H*, ^3J = 8.65 Hz, ^4J = 1.64 Hz), 6.80 (dd, 1H, Ar-*H*, ^3J = 8.35 Hz, ^4J = 1.64 Hz), 4.35 (q, 2H, $WCCH_2CH_3$, ^3J = 7.61 Hz), 2.44 (d, 3H, $(C_6H_5)_3PCH_3$, ^2J = 13.31 Hz), 2.16 (s, 3H, Ar−CH_3), 2.09 (s, 3H, Ar−CH_3′), 1.63 (s, 9H, $OC(CH_3)_3$), and 0.80 (t, 3H, $WCCH_2CH_3$, ^3J = 7.64 Hz) ppm. $^{31}P\{^1H\}$ NMR (C_6D_6, 121 MHz, 25 °C): δ = 21.8 ppm. $^{19}F\{^1H\}$ NMR (C_6D_6, 282 MHz, 25 °C): −69.38 (q, 3F, ^4J = 8.30 Hz), −71.24 (q, 3F, ^4J = 10.38 Hz), −74.08 (q, 3F, ^4J = 10.38 Hz), and −76.38 (q, 3F, ^4J = 8.30 Hz) ppm. Anal. Calcd for $C_{46}H_{44}F_{12}NO_3PW$ (1096.64 g/mol): C, 50.15; H, 4.03; N, 1.27. Found: C, 50.15; H, 3.96; N, 1.32.

[CF_3−ONO]W═C(CH_3)(Et)(O^tBu) (4). To a benzene (1 mL) solution of **3** (0.024 g, 2.1×10^{-5} mol) was added MeOTf (0.004 mg, 2.1×10^{-5} mol). The reaction solution turned immediately from red to brown and the solvent was removed in vacuo. The residue was dissolved in Et_2O and filtered to remove a colorless precipitate ($MePPh_3OTf$). The solvent was removed again in vacuo and the residue was dissolved in pentane and filtered. Removal off all volatiles from the filtrate provides **4** along with intractable impurities (<10%), thus precluding combustion analysis. Multinuclear and 2D NMR techniques provide the unambiguous characterization of **4** and the absolute assignment of all ^1H and $^{13}C\{^1H\}$ NMR resonances. ^1H NMR (C_6D_6, 500 MHz, 25 °C): δ = 7.67 (s, 1H, Ar-*H*), 7.65 (s, 1H, Ar-*H*), 6.76 (d, 1H, ^3J = 8.50 Hz, Ar-*H*), 6.71 (d, 1H, ^3J = 8.50 Hz, Ar-*H*), 6.61 (d, 1H, ^3J = 8.80 Hz, Ar-*H*), 6.51 (d, 1H, ^3J = 8.80 Hz, Ar-*H*), 4.87 (s, 3H, $WC(CH_3)CH_2CH_3$), 4.62 (m, 1H, WCHC(*H*′)(H)CH_3), 4.50 (m, 1H, WCHC(H′)(*H*)CH_3), 1.93 (s, 6H, CH_3), 1.19 (s, 9H, $OC(CH_3)_3$, and 0.70 (t, ^3J = 7.33 Hz, $WCHCH_2CH_3$) ppm. $^{19}F\{^1H\}$ NMR (C_6D_6, 470 MHz, 25 °C): δ = −76.3 (q, 3F, ^4J = 8.48 Hz), −75.6 (q, 3F, ^4J = 9.69 Hz), −71.1 (q, 3F, ^4J = 9.69 Hz), and −70.8 (q, 3F, ^4J = 8.48 Hz) ppm. $^{13}C\{^1H\}$ NMR (C_6D_6, 126 MHz, 25 °C): δ = 284.3 (s, $WC(CH_3)CH_2CH_3$), 145.3 (s, Ar *C*), 142.8 (s, Ar *C*), 134.2 (s, Ar *C*), 133.2 (s, Ar *C*), 131.9 (s, Ar *C*), 131.6 (s, Ar *C*), 127.3 (s, Ar *C*), 126.9 (s, Ar *C*), 126.5 (s, Ar *C*), 124.0 (s, Ar *C*), 122.8 (s, Ar *C*), 89.9 (s, -*OC*(CH_3)), 34.0 (s, $WC(CH_3)CH_2CH_3$), 29.1 (s, $OC(CH_3)_3$), 23.5 (s, $WC(CH_3)CH_2CH_3$), 20.4 (s, Ar-CH_3′), 20.2 (s, Ar-CH_3), and 18.4 (s, $WC(CH_3)CH_2CH_3$) ppm.

[CF_3−ONO]W═CH(Et)($OSiMe_3$) (5). To a diethyl ether (1 mL) solution of **3** (0.143 g, 1.30×10^{-4} mol) was added Me_3SiOTf (0.029 mg, 1.31×10^{-4} mol). The reaction solution turned immediately from red to brown and a colorless precipitate formed ($MePPh_3OTf$). The solid was removed by filtration and the filtrate was reduced to provide a brown oil. The product was immediately redissolved in C_6D_6 to prevent decomposition. The product was found to decompose when left as an oil for several hours, thus precluding combustion analysis. However, the complex was stable long enough in solution to be characterized by multinuclear and 2D NMR techniques, thus providing its unambiguous assignment. ^1H NMR (C_6D_6, 500 MHz, 25 °C): δ = 7.68 (s, 1H, Ar-*H*), 7.66 (s, 1H, Ar-*H*), 7.20 (t, 1H, W═C*H*CH_2CH_3, ^3J = 7.04 Hz), 6.71 (d, 1H, Ar-*H*, ^3J = 8.21 Hz), 6.61 (d, 1H, Ar-*H*, ^3J = 8.21 Hz), 6.53 (d, 1H, Ar-*H*, ^3J = 8.21 Hz), 6.51 (d, 1H, Ar-*H*, ^3J = 8.21 Hz), 5.28 (m, 1H, WCHC(H′)(*H*)CH_3), 4.91 (m, 1H, WCHC(*H*′)(H)CH_3), 1.97 (s, 3H, Ar−CH_3), 1.93 (s, 3H, Ar−CH_3′), 0.67 (t, 3H, $WCHCH_2CH_3$, ^3J = 7.33 Hz), and 0.12 (s, 9H, $OSi(CH_3)_3$) ppm. $^{19}F\{^1H\}$ NMR (C_6D_6, 470 MHz, 25 °C): −69.38 (q, 3F, ^4J = 9.61 Hz), −71.24 (q, 3F, ^4J = 9.61 Hz), −74.08 (q, 3F, ^4J = 9.61 Hz), and −76.38 (q, 3F, ^4J = 9.61 Hz) ppm. $^{13}C\{^1H\}$ NMR (C_6D_6, 126 MHz, 25 °C): δ = 262.1 (s, $WCHCH_2CH_3$), 145.8 (s, Ar *C*), 145.0 (s, Ar *C*), 134.5 (s, Ar *C*), 134.0 (s, Ar *C*), 132.0 (s, Ar *C*), 131.0 (s, Ar *C*), 127.2 (s, Ar *C*), 126.9 (s, Ar *C*), 126.4 (s, Ar *C*), 123.7 (s, Ar *C*), 123.6 (s, Ar *C*), 123.1 (s, Ar *C*), 31.3 (s, $WCHCH_2CH_3$), 20.6 (s, $WCHCH_2CH_3$), 20.2 (s, Ar-CH_3′), 20.0 (s, Ar-CH_3), and −0.1 (s, $OSi(CH_3)_3$) ppm.

Synthesis of [CF_3−ONO]W(O)(^{n}Pr) (6). To a 2.0 mL benzene solution of **2** (398 mg, 4.82×10^{-4} mol) was added trimethylsilyl triflate (1 mg, 4.5×10^{-6} mol) in benzene (1 mL). The solution changed from reddish-brown to aquamarine blue over the period of 2 h. The solution was evaporated in vacuo to remove solvent and trimethylsilyl triflate, providing an oil. Crystals of **6** formed from the oil after 3 h. The crystals were removed by spatula (0.274 g, 74.6%). ^1H NMR (C_6D_6, 300 MHz, 25 °C): δ = 7.52 (s, 2H, Ar-*H*), 6.73 (d, 1H, Ar-*H*, ^3J = 8.21 Hz), 6.68 (d, 1H, Ar-*H*, ^3J = 8.80 Hz), 6.61 (d, 1H, Ar-*H*, ^3J = 8.21 Hz), 6.52 (d, 1H, Ar-*H*, ^3J = 8.80 Hz), 3.03−2.97 (m, 2H, $WCH_2CH_2CH_3$), 2.81−2.52 (m, 2H, $WCH_2CH_2CH_3$), 1.92 (s, 3H, Ar−CH_3), 1.88 (s, 3H, Ar−CH_3), and 0.92 (t, 3H, $WCH_2CH_2CH_3$, ^3J = 7.33 Hz) ppm. $^{19}F\{^1H\}$ NMR (C_6D_6, 282 MHz, 25 °C): −71.17 (q, 3F, ^4J = 8.48 Hz), −71.77 (q, 3F, ^4J = 9.69 Hz), −75.55 (q, 3F, ^4J = 9.69 Hz), and −76.38 (q, 3F, ^4J = 8.48 Hz) ppm. $^{13}C\{^1H\}$ NMR (C_6D_6, 126 MHz, 25 °C): δ 146.5 (s, Ar), 145.5 (s, Ar), 135.5 (s, Ar), 133.9 (s, Ar), 132.8 (s, Ar−H), 127.5 (s, Ar−H), 125.4 (s, Ar), 123.0 (s, Ar−H), 82.7 (s, $WCH_2CH_2CH_3$, with satellites $^1J(^{13}C,^{183}W)$ = 109.1 Hz), 26.9 (s, $WCH_2CH_2CH_3$), 21.0 (Ar-−CH_3), 20.7 (s, $WCHCH_2CH_3$), and 19.3 (s, Ar-CH_3′) ppm. Anal. Calcd for $C_{24}H_{22}F_{12}NO_3W$ (769.22 g/mol): C, 36.76; H, 2.83; N, 1.79. Found: C, 36.67; H, 2.87; N, 1.79.

■ ASSOCIATED CONTENT

Ⓢ Supporting Information

^1H, $^{13}C\{^1H\}$, $^{31}P\{^1H\}$, 2-D NMR spectra, IR, and crystallographic data. This material is available free of charge via the Internet at http://pubs.acs.org/.

■ AUTHOR INFORMATION

Corresponding Author

veige@chem.ufl.edu

Notes

The authors declare no competing financial interest.

■ ACKNOWLEDGMENTS

This work was financially supported by UF, the Alfred P. Sloan Foundation, and the NSF in the form a CAREER award to A.S.V. (CHE-0748408). K.A.A. thanks UF and the NSF for funds to purchase X-ray equipment (CHE-0821346).

■ REFERENCES

(1) Odom, A. L. *Dalton Trans.* **2011**, *40*, 2689.
(2) Mindiola, D. J. *Acc. Chem. Res.* **2006**, *39*, 813.
(3) Firman, T. K.; Landis, C. R. *J. Am. Chem. Soc.* **2001**, *123*, 11728.
(4) Gordon, M. S.; Cundari, T. R. *Coord. Chem. Rev.* **1996**, *147*, 87.
(5) Nugent, W. A., James, M. *Mayer Metal−Ligand Multiple Bonds: The Chemistry of Transition Metal Complexes Containing Oxo, Nitrido, Imido, Alkylidene, or Alkylidyne Ligands*; Wiley: New York, 1988.
(6) Mindiola, D. J.; Bailey, B. C.; Basuli, F. *Eur. J. Inorg. Chem.* **2006**, 3135.

(7) Grubbs, R. H. *Handbook of Metathesis*; Wiley-VCH: Weinham, Germany, 2003; Vol. *1*−*3*.
(8) Tebbe, F. N.; Parshall, G. W.; Reddy, G. S. *J. Am. Chem. Soc.* **1978**, *100*, 3611.
(9) Scott, J.; Mindiola, D. J. *Dalton Trans.* **2009**, 8463.
(10) Hartley, R. C.; McKiernan, G. J. *J. Chem. Soc., Perkin Trans. 1* **2002**, 2763.
(11) Beckhaus, R.; Santamaria, C. *J. Organomet. Chem.* **2001**, *617*, 81.
(12) Flores, J. A.; Cavaliere, V. N.; Buck, D.; Pinter, B.; Chen, G.; Crestani, M. G.; Baik, M. H.; Mindiola, D. J. *Chem. Sci.* **2011**, *2*, 1457.
(13) Andino, J. G.; Fan, H. J.; Fout, A. R.; Bailey, B. C.; Baik, M. H.; Mindiola, D. J. *J. Organomet. Chem.* **2011**, *696*, 4138.
(14) Cavaliere, V. N.; Crestani, M. G.; Pinter, B.; Pink, M.; Chen, C. H.; Baik, M. H.; Mindiola, D. J. *J. Am. Chem. Soc.* **2011**, *133*, 10700.
(15) Fout, A. R.; Bailey, B. C.; Buck, D. M.; Tan, H. J.; Huffman, J. C.; Baik, M. H.; Mindiola, D. J. *Organometallics* **2010**, *29*, 5409.
(16) Bailey, B. C.; Fan, H. J.; Huffman, J. C.; Baik, M. H.; Mindiola, D. J. *J. Am. Chem. Soc.* **2007**, *129*, 8781.
(17) Bailey, B. C.; Tout, A. R.; Fan, H.; Tomaszewski, J.; Huffman, J. C.; Mindiola, D. J. *Angew. Chem., Int. Ed.* **2007**, *46*, 8246.
(18) Fout, A. R.; Bailey, B. C.; Tomaszewski, J.; Mindiola, D. J. *J. Am. Chem. Soc.* **2007**, *129*, 12640.
(19) Bailey, B. C.; Huffman, J. C.; Mindiola, D. J. *J. Am. Chem. Soc.* **2007**, *129*, 5302.
(20) Bailey, B. C.; Fout, A. R.; Fan, H. J.; Tomaszewski, J.; Huffman, J. C.; Gary, J. B.; Johnson, M. J. A.; Mindiola, D. J. *J. Am. Chem. Soc.* **2007**, *129*, 2234.
(21) Bailey, B. C.; Fan, H. J.; Baum, E. W.; Huffman, J. C.; Baik, M. H.; Mindiola, D. J. *J. Am. Chem. Soc.* **2005**, *127*, 16016.
(22) Adhikari, D.; Basuli, F.; Orlando, J. H.; Gao, X. F.; Huffman, J. C.; Pink, M.; Mindiola, D. J. *Organometallics* **2009**, *28*, 4115.
(23) Basuli, F.; Bailey, B. C.; Brown, D.; Tomaszewski, J.; Huffman, J. C.; Baik, M. H.; Mindiola, D. J. *J. Am. Chem. Soc.* **2004**, *126*, 10506.
(24) Schrock, R. R.; Czekelius, C. *Adv. Synth. Catal.* **2007**, *349*, 55.
(25) Tamm, M.; Wu, X. *Chim. Oggi-Chem. Today* **2010**, *28*, 60.
(26) Schrock, R. R. *Chem. Rev.* **2009**, *109*, 3211.
(27) Schrock, R. R.; Hoveyda, A. H. *Angew. Chem., Int. Ed.* **2003**, *42*, 4592.
(28) Wu, X. A.; Tamm, M. *Beilstein J. Org. Chem* **2011**, *7*, 82.
(29) Wu, X.; Daniliuc, C. G.; Hrib, C. G.; Tamm, M. *J. Organomet. Chem.* **2011**, *696*, 4147.
(30) Haberlag, B.; Wu, X.; Brandhorst, K.; Grunenberg, J.; Daniliuc, C. G.; Jones, P. G.; Tamm, M. *Chem.—Eur. J.* **2010**, *16*, 8868.
(31) Beer, S.; Brandhorst, K.; Hrib, C. G.; Wu, X.; Haberlag, B.; Grunenberg, J.; Jones, P. G.; Tamm, M. *Organometallics* **2009**, *28*, 1534.
(32) Beer, S.; Hrib, C. G.; Jones, P. G.; Brandhorst, K.; Grunenberg, J.; Tamm, M. *Angew. Chem., Int. Ed.* **2007**, *46*, 8890.
(33) Zhang, W.; Kraft, S.; Moore, J. S. *Chem. Commun.* **2003**, 832.
(34) Poater, A.; Solans-Monfort, X.; Clot, E.; Coperet, C.; Eisenstein, O. *J. Am. Chem. Soc.* **2007**, *129*, 8207.
(35) Schrock, R. R.; Jamieson, J. Y.; Araujo, J. P.; Bonitatebus, P. J.; Sinha, A.; Pia, L.; Lopez, H. *J. Organomet. Chem.* **2003**, *684*, 56.
(36) Cochran, F. V.; Schrock, R. R. *Organometallics* **2001**, *20*, 2127.
(37) Shih, K. Y.; Totland, K.; Seidel, S. W.; Schrock, R. R. *J. Am. Chem. Soc.* **1994**, *116*, 12103.
(38) Kempf, B.; Hampel, N.; Ofial, A. R.; Mayr, H. *Chem.—Eur. J.* **2003**, *9*, 2209.
(39) *The Chemistry of Enamines*; Rapport, Z., Ed.; John Wiley & Sons, Inc.: New York, 1994.
(40) *Enamines: Synthesis, Structure, And Reactivity*; Cook, A. G., Ed.; Marcel Dekker, Inc.: New York, 1988.
(41) Jensen, K. L.; Dickmeiss, G.; Jiang, H.; Albrecht, L.; Jorgensen, K. A. *Acc. Chem. Res.* **2012**, *45*, 248−264.
(42) Kano, T.; Maruoka, K. *Bull. Chem. Soc. Jpn.* **2010**, *83*, 1421.
(43) Palomo, C.; Oiarbide, M.; Lopez, R. *Chem. Soc. Rev.* **2009**, *38*, 632.
(44) Xu, L.-W.; Li, L.; Shi, Z.-H. *Adv. Synth. Catal.* **2010**, *352*, 243.
(45) Xu, L.-W.; Lu, Y. *Org. Biomol. Chem.* **2008**, *6*.
(46) Sarkar, S.; McGowan, K. P.; Culver, J. A.; Carlson, A. R.; Koller, J.; Peloquin, A. J.; Veige, M. K.; Abboud, K. A.; Veige, A. S. *Inorg. Chem.* **2010**, *49*, 5143.
(47) Koller, J.; Sarkar, S.; Abboud, K. A.; Veige, A. S. *Organometallics* **2007**, *26*, 5438.
(48) Sarkar, S.; Carlson, A. R.; Veige, M. K.; Falkowski, J. M.; Abboud, K. A.; Veige, A. S. *J. Am. Chem. Soc.* **2008**, *130*, 1116.
(49) Golisz, S. R.; Labinger, J. A.; Bercaw, J. E. *Organometallics* **2010**, *29*, 5026.
(50) Agapie, T.; Day, M. W.; Bercaw, J. E. *Organometallics* **2008**, *27*, 6123.
(51) Agapie, T.; Bercaw, J. E. *Organometallics* **2007**, *26*, 2957.
(52) O'Reilly, M.; Falkowski, J. M.; Ramachandran, V.; Pati, M.; Abboud, K. A.; Dalal, N. S.; Gray, T. G.; Veige, A. S. *Inorg. Chem.* **2009**, *48*, 10901.
(53) McGowan, K. P.; Abboud, K. A.; Veige, A. S. *Organometallics* **2011**, *30*, 4949.
(54) McGowan, K. P.; Veige, A. S. *J. Organomet. Chem.* **2012**, accepted.
(55) Golisz, S. R.; Bercaw, J. E. *Macromolecules* **2009**, *42*, 8751.
(56) Sarkar, S.; McGowan, K. P.; Kuppuswamy, S.; Ghiviriga, I.; Abboud, K. A.; Veige, A. S. *J. Am. Chem. Soc.* **2012**, *123*, 4509−4512.
(57) Jan, M. T.; Sarkar, S.; Kuppuswamy, S.; Ghiviriga, I.; Abboud, K. A.; Veige, A. S. *J. Organomet. Chem.* **2011**, *696*, 4079.
(58) O'Reilly, M. E.; Del Castillo, T. J.; Abboud, K. A.; Veige, A. S. *Dalton Trans.* **2012**, *41*, 2237.
(59) Sarkar, S.; Abboud, K. A.; Veige, A. S. *J. Am. Chem. Soc.* **2008**, *130*, 16128.
(60) O'Reilly, M. E.; Del Castillo, T. J.; Falkowski, J. M.; Ramachandran, V.; Pati, M.; Correia, M. C.; Abboud, K. A.; Dalal, N. S.; Richardson, D. E.; Veige, A. S. *J. Am. Chem. Soc.* **2011**, *133*, 13661.
(61) Lu, F.; Zarkesh, R. A.; Heyduk, A. F. *Eur. J. Inorg. Chem.* **2012**, 467.
(62) Heyduk, A. F.; Zarkesh, R. A.; Nguyen, A. I. *Inorg. Chem.* **2011**, *50*, 9849.
(63) Nguyen, A. I.; Zarkesh, R. A.; Lacy, D. C.; Thorson, M. K.; Heyduk, A. F. *Chem. Sci* **2011**, *2*, 166.
(64) Zarkesh, R. A.; Heyduk, A. F. *Organometallics* **2011**, *30*, 4890.
(65) Corey, J. Y.; Trankler, K. A.; Braddock-Wilking, J.; Rath, N. P. *Organometallics* **2010**, *29*, 5708.
(66) Schrock, R. R.; Listemann, M. L.; Sturgeoff, L. G. *J. Am. Chem. Soc.* **1982**, *104*, 4291.
(67) Kuppuswamy, S.; Peloquin, A. J.; Ghiviriga, I.; Abboud, K. A.; Veige, A. S. *Organometallics* **2010**, *29*, 4227.
(68) Oskam, J. H.; Schrock, R. R. *J. Am. Chem. Soc.* **1993**, *115*, 11831.
(69) Oskam, J. H.; Schrock, R. R. *J. Am. Chem. Soc.* **1992**, *114*, 7588.
(70) Tonzetich, Z. J.; Schrock, R. R.; Muller, P. *Organometallics* **2006**, *25*, 4301.
(71) Schrock, R. R.; Shih, K.-Y.; Dobbs, D. A.; Davis, W. M. *J. Am. Chem. Soc.* **1995**, *117*, 6609.
(72) Youinou, M. T.; Kress, J.; Fischer, J.; Aguero, A.; Osborn, J. A. *J. Am. Chem. Soc.* **1988**, *110*, 1488.
(73) Bryan, J. C.; Mayer, J. M. *J. Am. Chem. Soc.* **1987**, *109*, 7213.
(74) Boyd, P. D. W.; Glenny, M. G.; Rickard, C. E. F.; Nielson, A. J. *Polyhedron* **2011**, *30*, 632.
(75) Rosenfeld, D. C.; Kuiper, D. S.; Lobkovsky, E. B.; Wolczanski, P. T. *Polyhedron* **2006**, *25*, 251.
(76) Clough, C. R.; Greco, J. B.; Figueroa, J. S.; Diaconescu, P. L.; Davis, W. M.; Cummins, C. C. *J. Am. Chem. Soc.* **2004**, *126*, 7742.
(77) Lentz, M. R.; Vilardo, J. S.; Lockwood, M. A.; Fanwick, P. E.; Rothwell, I. P. *Organometallics* **2004**, *23*, 329.
(78) Veige, A. S.; Slaughter, L. M.; Lobkovsky, E. B.; Wolczanski, P. T.; Matsunaga, N.; Decker, S. A.; Cundari, T. R. *Inorg. Chem.* **2003**, *42*, 6204.
(79) Lehtonen, A.; Sillanpaa, R. *Polyhedron* **2002**, *21*, 349.
(80) Kramkowski, P.; Baum, G.; Radius, U.; Kaupp, M.; Scheer, M. *Chem.—Eur. J.* **1999**, *5*, 2890.

(81) Chen, T. N.; Wu, Z. Z.; Li, L. T.; Sorasaenee, K. R.; Diminnie, J. B.; Pan, H. J.; Guzei, I. A.; Rheingold, A. L.; Xue, Z. L. *J. Am. Chem. Soc.* **1998**, *120*, 13519.
(82) ODonoghue, M. B.; Schrock, R. R.; LaPointe, A. M.; Davis, W. M. *Organometallics* **1996**, *15*, 1334.
(83) Nugent, W. A.; Feldman, J.; Calabrese, J. C. *J. Am. Chem. Soc.* **1995**, *117*, 8992.
(84) Arnaudet, L.; Bougon, R.; Buu, B.; Lance, M.; Nierlich, M.; Vigner, J. *Inorg. Chem.* **1993**, *32*, 1142.
(85) Chisholm, M. H.; Cook, C. M.; Folting, K.; Streib, W. E. *Inorg. Chim. Acta* **1992**, *198*, 63.
(86) Leny, J. P.; Youinou, M. T.; Osborn, J. A. *Organometallics* **1992**, *11*, 2413.
(87) Legzdins, P.; Rettig, S. J.; Ross, K. J.; Veltheer, J. E. *J. Am. Chem. Soc.* **1991**, *113*, 4361.
(88) Arnaudet, L.; Bougon, R.; Ban, B.; Charpin, P.; Isabey, J.; Lance, M.; Nierlich, M.; Vigner, J. *Inorg. Chem.* **1989**, *28*, 257.
(89) Bryan, J. C.; Mayer, J. M. *J. Am. Chem. Soc.* **1987**, *109*, 7213.
(90) Feinsteinjaffe, I.; Gibson, D.; Lippard, S. J.; Schrock, R. R.; Spool, A. *J. Am. Chem. Soc.* **1984**, *106*, 6305.
(91) Churchill, M. R.; Rheingold, A. L. *Inorg. Chem.* **1982**, *21*, 1357.
(92) Churchill, M. R.; Missert, J. R.; Youngs, W. J. *Inorg. Chem.* **1981**, *20*, 3388.
(93) Bassi, I. W.; Scordamaglia, R. *J. Organomet. Chem.* **1975**, *99*, 127.
(94) Tonzetich, Z. J.; Lam, Y. C.; Müller, P.; Schrock, R. R. *Organometallics* **2007**, *26*, 475.
(95) Warren, T. H.; Schrock, R. R.; Davis, W. M. *J. Organomet. Chem.* **1998**, *569*, 125.
(96) Geyer, A. M.; Wiedner, E. S.; Gary, J. B.; Gdula, R. L.; Kuhlmann, N. C.; Johnson, M. J. A.; Dunietz, B. D.; Kampf, J. W. *J. Am. Chem. Soc.* **2008**, *130*, 8984.
(97) Schrock, R. R.; Hoveyda, A. H. *Angew. Chem., Int. Ed.* **2003**, *42*, 4592.
(98) Freudenberger, J. H.; Schrock, R. R. *Organometallics* **1985**, *4*, 1937.
(99) Becke, A. D. *J. Chem. Phys.* **1993**, *98*, 5648.
(100) Lee, C.; Yang, W.; Parr, R. G. *Phys. Rev. B: Condens. Matter* **1988**, *37*, 785.
(101) Frisch, M. J.; Trucks, G.; Schlegel, H. B.; Scuseria, G. E.; Robb, M. A.; Cheeseman, J. R.; Scalmani, G.; Barone, V.; Mennucci, B.; Petersson, G. A.; Nakatsuji, H.; Caricato, M.; Li, X.; Hratchian, H. P.; Izmaylov, A. F.; Bloino, J.; Zheng, G.; Sonnenberg, J. L.; Hada, M.; Ehara, M.; Toyota, K.; Fukuda, R.; Hasegawa, J.; Ishida, M.; Nakajima, T.; Honda, Y.; Kitao, O.; Nakai, H.; Vreven, T.; Montgomery, J. A.; Peralta, J. E.; Ogliaro, F.; Bearpark, M.; Heyd, J. J.; Brothers, E.; Kudin, K. N.; Staroverov, V. N.; Kobayashi, R.; Normand, J.; Raghavachari, K.; Rendell, A.; Burant, J. C.; Iyengar, S. S.; Tomasi, J.; Cossi, M.; Rega, N.; Millam, J. M.; Klene, M.; Knox, J. E.; Cross, J. B.; Bakken, V.; Adamo, C.; Jaramillo, J.; Gomperts, R.; Stratmann, R. E.; Yazyev, O.; Austin, A. J.; Cammi, R.; Pomelli, C.; Ochterski, J. W.; Martin, R. L.; Morokuma, K.; Zakrzewski, V. G.; Voth, G. A.; Salvador, P.; Dannenberg, J. J.; Dapprich, S.; Daniels, A. D.; Farkas, O.; Foresman, J. B.; Ortiz, J. V.; Cioslowski, J.; Fox, D. J. *Gaussian 09, Revision A.02*; Gaussian: Wallingford, CT, 2009.
(102) Hay, P. J.; Wadt, W. R. *J. Chem. Phys.* **1985**, *82*, 270.